Materials Chemistry and Physics 308 (2023) 128265



Contents lists available at ScienceDirect

Materials Chemistry and Physics

journal homepage: www.elsevier.com/locate/matchemphys



Enhancing antibacterial and anticorrosive properties of 316L stainless steel with nanocoating of copper oxide nanoparticles

Gizem Karabulut [a,*], Nuray Beköz Üllen [a], Selcan Karakuş [b], Ceyhun Toruntay [c]

[a] Istanbul University-Cerrahpaşa, Faculty of Engineering, Departmant of Metallurgical and Material Engineering, İstanbul, Turkey
[b] Istanbul University-Cerrahpaşa, Faculty of Engineering, Departmant of Chemistry, İstanbul, Turkey
[c] Istanbul Technical University, Faculty of Science and Letters, Department of Molecular Biology and Genetics, İstanbul, Turkey

HIGHLIGHTS

- 316 L stainless steel coated with Mat/PEG-CuO NPs.
- Improved anticorrosive property was evaluated.
- Antibacterial activity against *S. aureus* and *E. coli.*
- Multifunctional CuO NPs for biomedical application.

ARTICLE INFO

Keywords:
Copper oxide nanoparticles
Surface modification
Multifunctional coating
Environmentally friendly

ABSTRACT

Surface modifications are frequently applied to enhance the multifunctional performance of metallic materials in biomedical applications, and nanotechnology has the advantage of enabling the development of highly customized surface functions and properties. However, the surface of 316L stainless steel (SS316L) exhibits bioinert behavior with tissues, can be easily corroded by body fluids due to the containing Cl^- ions, and leads to bacterial attachment. This study aimed to improve the multifunctional properties of SS316L by coating it with a novel matcha/polyethylene glycol-CuO NPs (Mat/PEG-CuO NPs) synthesized by a simple ultrasound-assisted method. The phyto/sonosynthesized CuO NPs were characterized by a range of advanced techniques, and their coating on the surface of SS316L was analyzed for electrochemical corrosion and antibacterial behavior. The experimental results showed that the spherical-shaped CuO NPs were successfully fabricated and coated onto SS316L to improve its surface characteristics. The coating with CuO NPs, having an average thickness of 5.31 μm, demonstrated exceptional anti-corrosive and anti-bacterial characteristics, showing a zone of inhibition measuring 29.5 mm and 25.5 mm against *Escherichia coli* (*E. coli*) and *Staphylococcus aureus* (*S. aureus*), respectively. The results demonstrate the successful fabrication of spherical CuO NPs coated onto SS316L, which holds great promise for biomedical applications.

1. Introduction

Stainless steel type SS316L, known for its attractive properties including high toughness, non-magnetic, machinability, and hardenability properties, as well as its easy availability and cost-effectiveness, is widely utilized in medical applications [1–4]. However, SS316L is bioinert to body tissues, bacteria can easily attach to its surface, and leading to corrosion upon contact with body fluids [4,5]. To reduce or eliminate these negative properties, surface modification of biometallic materials by coating is an effective, simple, and applicable method [6]. In recent years, coating the surface of biometallic materials with multifunctional metal-based nanoparticles (MNPs) has been a widely studied subject [7–14]. MNPs are presently composed of elemental metals (metal NPs) or metallic compounds (metal oxide NPs). MNPs are preferred for coating implant surfaces because their nanoscale structures are less toxic than the macroscale, their properties increase due to the

* Corresponding author. Istanbul University-Cerrahpaşa, Engineering Faculty, Metallurgical and Materials Engineering Department, 34320, Avcılar, İstanbul, Turkey.
E-mail addresses: gizem.karabulut@iuc.edu.tr (G. Karabulut), nbekoz@iuc.edu.tr (N. Beköz Üllen), selcan@iuc.edu.tr (S. Karakuş), ctoruntay@itu.edu.tr (C. Toruntay).

https://doi.org/10.1016/j.matchemphys.2023.128265
Received 18 April 2023; Received in revised form 17 July 2023; Accepted 28 July 2023
Available online 29 July 2023
0254-0584/© 2023 Elsevier B.V. All rights reserved.

higher surface area, and they provide multifunctional properties to the surface of the implant. CuO NPs are a popular choice for coating implant surfaces due to their properties as p-type semiconductors with a band gap of 1.7 eV, as well as their multifunctional capabilities in terms of electromagnetic, photonic, and physical characteristics. Their nanoscale size offers a greater surface area, which is desirable for achieving the desired properties, and they are considered a flexible material for various applications, as they are less toxic at the nanoscale level compared to the macroscopic level [15–19]. In recent literature, there has been significant attention given to the toxicity of Cu-based materials. Lin et al. reported a comprehensive study using large-scale screening assays to rank the toxicity of various Cu-based NPs. The results of their research showed a clear toxicity trend, with $CuCl_2$ (0.1 mg/L) > nCu (0.25 mg/L) > nCu(OH)$_2$-a = nCu(OH)$_2$-ab (0.3 mg/L) > nCuO (0.5 mg/L) > μCu = μCuO (≥1 mg/L) based on a zebrafish embryo HTS assay. According to their findings, Cu^{2+} exhibited the highest level of toxicity, followed by nano-Cu, nano-CuO, nano-Cu(OH)$_2$, micro-Cu, and micro-CuO [20]. In another study, Lin et al. [21], examined the toxicological effects of ZnO, CuO, Co_3O_4, and NiO metal oxides in zebrafish embryos and early larvae. When the toxicity of these oxides was examined, it showed an ion release and toxicity as ZnO, NiO, CuO, and Co_3O_4 respectively. It has been stated that especially NiO and CuO vary depending on dose and time and should be examined. In addition, it was stated in the study that the toxic effect could be reduced. This is advantageous in that CuO NPs can be used. Moreover, prior research has indicated the potential to mitigate the toxic effects associated with CuO NPs, thereby enhancing their suitability for diverse applications. Zhang et al. [22] conducted an independent investigation into the toxicity behavior of various metal oxides and revealed that the toxicity of CuO NPs can be regulated by manipulating their solubility behavior. Adeleye et al. [23] and Naatz et al. [24], in their respective studies, further emphasized the influence of iron (Fe) doping on the solubility behavior of CuO NPs, thereby facilitating the control of their toxicity.

Due to their antibacterial behavior [25], photocatalysis properties [26], and anti-fouling [27] at the nanoscale, CuO NPs are a preferred alternative for surface coatings. Moreover, the phytosynthesis of CuO NPs is highly favored in biomedical applications due to their complete compatibility and eco-friendly production method. Green nanotechnology offers an environmentally sustainable and cost-effective approach to developing novel nanostructures using of plant extracts. The literature contains numerous studies on the phytofabrication of CuO NPs, which have demonstrated their positive results in biocompatibility tests, including antibacterial, antioxidant, anticancer, and cytotoxic activity [16,28–31]. In various studies, it has been reported that when polymer solutions/blends and metal oxide nanoparticles (MO NPs) exhibit a thermodynamic compatibility with the polymer matrix by calculating the Flory-Huggins interaction parameters [32–37]. It is possible to assess how well MO NPs interact with a polymer matrix without causing significant phase separation or aggregation by utilizing the commonly used Flory-Huggins theory, which is employed to characterize nanostructures. This compatibility is crucial as it allows for the synergistic combination of the distinct characteristics of both the biopolymer and metal oxide nanoparticles, resulting in the development of surface properties, coatings, and material functions that meet desired modifications.

Post-implant reactions are a significant risk in surgical applications following the implantation of metallic materials. Additionally, the formation of bacterial species that are resistant to traditional treatments due to the increasing use of antibiotics has become a global problem, alongside biofilm formation and inflammation problems on the surface of metallic implants [38]. Hence, there is a need to develop new antibacterial agents to reduce the use of antibiotics and mitigate these issues. Post-implant reaction related pathogens generally are *Staphylococcus aureus* (*S. aureus*), *Pseudomonas aeruginosa* (*P. aureginosa*), *and Escherichia coli* (*E. coli*) [39,40].

Corrosion is a significant issue in the use of metallic materials as

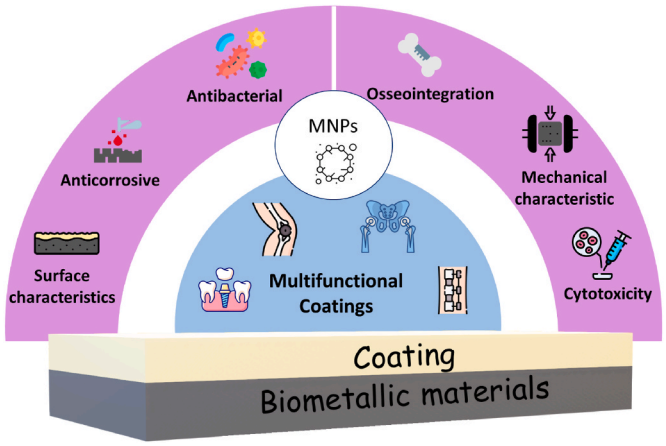


Fig. 1. Biocompatibility tests applied to MNPs coating.

biomaterials. Despite SS316L's high corrosion resistance, when exposed to corrosive body fluids, various toxic and allergenic effects can arise from the formation of corrosion products such as nickel, chromium, and cobalt elements and their compounds [41]. To address this issue, several surface modification techniques, such as electrodeposition, sol-gel coating, and chemical vapor deposition, are applied to metallic materials to improve their surface properties [42–44]. Many investigations have focused on the surface modification of biometals, from various perspectives. The deterioration in implant material surface properties varies depending on factors such as the type of implant, its usage area, and the area's movement. Numerous studies have aimed to improve the biocompatibility and surface properties of implant materials [45–47]. Enhancing the surface properties of these materials is crucial, and one promising approach is to use CuO NPs synthesized through phytofabrication strategies. These metal oxide NPs provide multifunctional attributes to the surface through nanoscale modification. CuO is widely used in various fields, including catalysts, sensors, antimicrobial agents, and superconducting materials [48]. CuO NPs are considered more economical to produce compared to gold (Au) and silver (Ag) NPs, and they have potent antimicrobial properties due to their characteristic crystal structure. Several studies have reported the effective antimicrobial behavior of CuO NPs against *E. coli* and *S. aureus*, depending on the concentration and particle size [49–51]. However, there are very few studies in the literature on coating SS316L surfaces with CuO NPs. One study by Tavakoli et al. [25] investigated the anticorrosive and antibacterial behavior of 316 L stainless steel by incorporating CuO NPs into polydimethylsiloxane (PDMS) and reported the presence of CuO NPs in the coating improved its antibacterial and anticorrosive behavior. Due to the widespread use of CuO NPs coatings for both industrial and academic applications, multi-faceted investigation of their potential biological and environmental effects has become important. The investigation of MNPs is highly prone to interdisciplinary study. The potential influences of the presence of CuO NPs the biocompatibility is an important design criterion for CuO NPs use in human life. Various characterization methods applied to MNPs coatings to determine the biocompatibility are given in Fig. 1. Therefore, this study aims to address lack of knowledge in the literature by preparing a Mat/PEG-CuO NPs bionanocomposite coating material and investigating its physicochemical properties, as well as its anticorrosive and antibacterial effects on SS316L surfaces. The wide, successful application of CuO NPs is attributable to their distinct biocompatibility performance. In the continuation of the study, it is aimed to carry out characterization studies that complete the biocompatibility on the right side of Fig. 1.

Multifaceted research is necessary to enhance the productivity of CuO NP coating on metallic surfaces and to comprehend their surface characteristics. In the current study, a coating were performed with CuO NPs which synthesized using matcha extract, onto the surface of SS316L

Table 1
The chemical compound of SS316L.

C	Ni	Cr	Mo	Si	Mn	Cu	S	P	N	Fe
0,014	10,091	16,581	2048	0,437	1317	0,326	0024	0,025	0041	Balance

to enhance its antibacterial and anticorrosive properties. This is the first report in the literature on using matcha extract-based synthesized CuO NPs for coating SS316L. To achieve this, CuO NPs were synthesized through phyto/sonofabrication-assisted synthesis and characterized their chemical, physical, and surface properties. The airbrush spray coating method was used to coat the phyto/sonosynthesized CuO NPs onto the surface of SS316L. The coated surface was then evaluated for morphological features, surface roughness, thickness, coating distribution analysis, and antibacterial and anticorrosive behavior using disc diffusion and electrochemical polarization tests. Our study presents a novel coating technique, and the results suggest that the CuO NPs coated SS316L has promising qualitative corrosion and antibacterial properties, making it suitable for medical applications. This study fills a gap in the literature by providing a comprehensive understanding of the phyto/sonosynthesis and coating of CuO NPs on SS316L and can guide future studies in this area. Thus, this study is significant in providing direction and insight to other researchers in this field.

2. Materials and methods

2.1. Materials

The Matcha tea powder, which is a member of the *Camellia sinensis* family, was purchased from Arifoğlu Company based in Turkey. Copper (II) sulfate pentahydrate ($CuSO_4{\cdot}5H_2O$), sodium hydroxide (NaOH) (molecular weight: 40.00 g/mol), and ethanol (EtOH, purity ≥%99.4) was supplied from Merck Company based in Germany. Polyethylene glycol (PEG) (molecular weight: 400 kDa) was purchased from Fluka based in Switzerland. SS316L was provided by Birçelik Company (Turkey) and had a 28 mm diameter along with a length of 1 m. The chemical compound of SS316L is presented in Table 1.

2.2. Preparation of Mat/PEG-CuO NPs

The phyto/sono-based method, which is an environmentally friendly, low-cost, effective, and fast method, was used for the phyto/sonosynthesis of CuO NPs with biopolymeric matrix. The first step in the preparation of biopolymeric matrix CuO NPs is the preparation of the plant extract. After washing several times with distilled water and drying in a vacuum oven at 50 °C for 2 h, 5 g of the prepared matcha tea was added to 100 mL of distilled water. The sample was kept in a sterile, dark container at 27 °C for three days. Afterwards, it was decanted and filtered using coarse filter paper to obtain the matcha extract (Mat). To create a Mat/PEG blend, 0.1 g of PEG was added to the Mat solution. Next, 0.0424 g of $CuSO_4{\cdot}5H_2O$ was dissolved in distilled water (50 mL) and mixed with the prepared Mat/PEG solution. Separately, 0.2 g of NaOH was dissolved in distilled water (50 mL) and stirred at room temperature for 10 min. The NaOH solution was added dropwise to the mixture using a Pasteur pipette and stirred for an additional 10 min. Finally, the mixture was sonicated at 50% amplitude for 30 min and filtered through a sterile 0.22-μm filter. The resulting solution was stored in a sterile container in the dark at room temperature for use in experimental studies.

2.3. Coating of SS316L with Mat/PEG-CuO NPs

SS316L bar (28 mm diameter and 1 m length) was sliced to 2 mm thickness by computer numerical control (CNC) cutting process. After the cutting process, the substrate materials are 25 mm in diameter. Before starting the coating process, a 10 min ultrasonic bath was performed in an ethanol-acetone mixture to remove impurities such as cutting fluid, oil, dirt, and dust that may remain on the surface. After drying (10 min, 60 °C), the parts were coated using the airbrush spray method. A piston type of airbrush compressor kit (model: AS186) is used for the coating process. The prepared Mat/PEG-CuO NPs solution was sprayed from a distance of 75 mm at 3 bar and for 4 s. The schematic overview of the experimental steps is presented in Fig. 2.

2.4. Characterization

In this study, the phyto/sonosynthesized Mat/PEG-CuO NPs solution was characterized by ultraviolet visible spectrophotometry (UV–Vis),

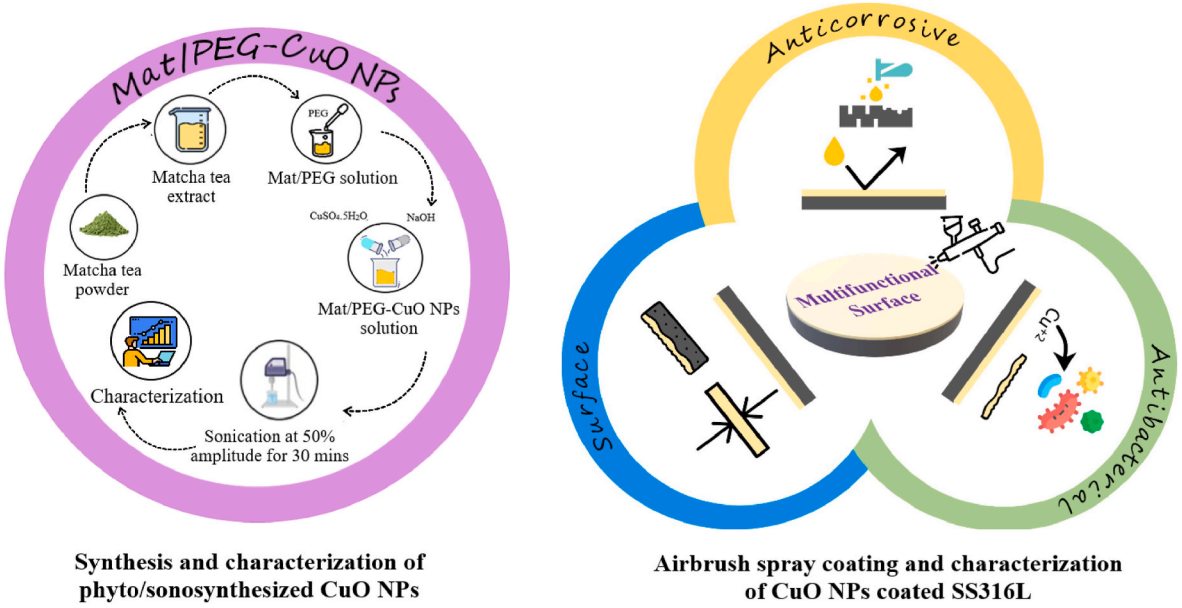


Fig. 2. Schematic overview of the experimental study.

Fourier transform infrared (FTIR) spectroscopy, X-ray diffraction (XRD), scanning electron microscopy (SEM), and transmission electron microscope (TEM). The absorbance measurements were performed with a PG Instruments T + 80 model dual-beam UV–Vis spectrophotometer using UVWin 5 software. The functional group analysis of the pure Mat and Mat/PEG-CuO NPs were performed on a PerkinElmer Spectrum Two model device with a frequency range of 4000–400 cm^{-1}. In order to examine the crystalline structure of the phyto/sonosynthesized biopolymeric matrix CuO NPs, the Rigaku D/Max2200/PC XRD device, which can scan between 20° and 80° with a Cu-Kα beam at 40 kV and 15 mA, was used. Zeiss-Sigma 300 SEM and Hitachi High Tech HT7700 TEM (at 100 kV) devices were used to determine the properties of Mat/PEG-CuO NPs such as surface morphology, shape, size, and distribution. By using Debye-Scherrer Equation with the data obtained from XRD analysis, the crystalline size of Mat/PEG-CuO NPs can be calculated (Eq. (2.1)).

$$D_p = \frac{0.94.\lambda}{\beta.cos\,\theta} \quad (2.1)$$

where K is the shape factor (0.9), D is the crystalline size, β is the full width at half maximum (FWHM) of the peak, λ is the X-ray wavelength (0.15406), and θ is the Bragg angle.

The coated samples underwent various forms of analysis to determine their properties. These included SEM, optical microscopy, average surface roughness, and profilometer measurements. The SEM analysis was conducted using a Zeiss-Sigma 300 device to observe the distribution, size, and morphology of NPs on the surface of SS316L coated with Mat/PEG-CuO NPs by airbrush spray method. The optical microscope used for the structure of coating and thickness measurements was a Nikon brand Eclipse MA100 model. An electrolytic etching process was employed using a 30% NaOH-distilled water solution for 5 s. Mitutoyo (Surftest SJ-210) device was used to analyze the average surface roughness of both coated and uncoated specimens. Using a profilometer (KLA Tencor Stylus Profiler P7), the distribution and thickness of the Mat/PEG-CuO NPs coating on the surface of SS316L were investigated.

2.5. Electrochemical corrosion test

A computer-connected potentiostat (Gamry, Interface 1000) was used to understand the effect of Mat/PEG-CuO NPs coatings on the corrosion properties of SS316L. To examine the electrochemical corrosion properties of the specimens, tests were carried out in a 1000 mL cell containing Ringer's solution at pH 7. A conventional three-electrode system was employed in the testing process. Software such as Framework and Echem Analyst Gamry were used for data analysis. The open circuit potential (OCP) measurements of both the uncoated and coated samples were carried out initially. After obtaining stable OCP curves, cyclic polarization was applied to the samples. Tafel measurements were performed with polarizing the electrochemical corrosion test samples from - 250 mV vs. OCP to +250 mV vs. OCP at a scanning rate of 1.0 mV/min.

2.6. Antibacterial activity test

The agar well diffusion technique was employed to evaluate the antibacterial activities of coated and uncoated specimens. *E. coli* was preferred as a gram-negative bacteria and *S. aureus* was preferred as a gram-positive bacteria. Once the freshly started culture reached OD_{600}, 75 μL of each bacteria culture were separately spread onto Tryptic Soy Broth (TSB)-agar plates that were previously prepared. Subsequently, the coated and uncoated specimens were placed on the plates, and were incubated at 37 °C for 16 h. Following the incubation period, the zones of inhibition (ZOI) that formed around the specimens on the plates were measured on a non-reflective black surface using a ruler.

3. Results and discussion

3.1. Characterization result of Mat/PEG-CuO NPs

UV–Vis analysis is a fundamental method for the characterization of NPs, with agglomeration and dispersion affecting their optical properties, leading to variations in absorbance values. The UV–Vis spectrum of ultrasound-assisted plant-mediated synthesized CuO NPs with matcha tea extract and PEG is shown in Fig. 3a. Mat/PEG-CuO NPs formed a spectrum that started at 600 nm and peaked at 810 nm, potentially due to surface plasmon resonance (SPR). SPR results from the surface electron oscillation of NPs, and the prepared NPs' shape is highly correlated to the high detected spectra [52]. Since various factors determine the shape of NPs, such differences are acceptable. A broad peak signifies that the particles have a polydisperse distribution [53]. The functional groups of the matcha extract and Mat/PEG-CuO NPs were investigated with the FTIR technique. In Fig. 3b, FTIR results of matcha extract typical peaks were observed at 3282.25 cm^{-1} (-OH stretching vibration), 2979.48 cm^{-1} (asymmetric $-CH_2$ vibration), 2918.73 cm^{-1} (asymmetric $-CH_2$ vibration), 1627.63 cm^{-1} (-OH stretching vibration), 1517.70 cm^{-1} (C═O stretching vibration), 1446.35 cm^{-1} (C═O stretching vibration), 1373.07 cm^{-1} (C═O stretching vibration), 1235.18 cm^{-1} (C–OH bending), 1144.54 cm^{-1} (C–OH bending), and 1014.37 cm^{-1} (C–*O*–C stretching vibration) [54,55]. The FTIR spectra of the phyto/-sonosynthesized Mat/PEG-CuO NPs were formed at 3329.50 cm^{-1} (-OH stretching vibration), 2980.45 cm^{-1} (asymmetric $-CH_2$ vibration), 1617.12 cm^{-1} (C═O stretching vibration), 1385.61 cm^{-1} (C–N vibration), and 1093.44 cm^{-1} (C–O vibration). In addition to these peaks, Cu–O stretching vibration peaks formed at 943.02 cm^{-1}, 834.06 cm^{-1}, 763.67 cm^{-1}, 659.54 cm^{-1}, and 592.04 cm^{-1} [28,55]. In the literature, it has been reported that in the presence of metal ions, PEG derivatives or components of tea extract can bind to metal ions through chelating agents and donor atoms such as oxygen and nitrogen, forming chelate complexes [56]. According to our experimental results, it indicates that both polyethylene glycol (PEG) and tea extract can function as chelating agents in the context of obtaining green CuO NPs by shifting the peaks associated with hydroxyl groups (OH), carbonyl groups (C═O), and aromatic rings. Thus, they can bind to metal ions such as Cu^{2+} and assist in the formation and stabilization of Mat/PEG-CuO NPs. Fig. 3c shows the XRD spectra of phyto/sonosynthesized Mat/PEG-CuO NPs. The major characteristic peaks at 31.5°(110), 39.5°(111), 45.4°(202), 47.3° (−202), 56.3°(020), and 75.1°(22–2), were indexed to the monoclinic geometry of the CuO tenorite structure as referenced against the JCPDS 80–1268 [16,57,58]. The peak position were slightly sifted to lower-angle compared to those noted in literature owing to integration of the polymeric phase within the CuO NPs. The peaks occurring at 2θ = 25.5°, 28.3° and 29.4° are due to organic structures in the matrix phase. The crystal size of phyto/sonosynthesized CuO NPs calculated using **Eq. (2.1).** and it was found to be 33.17 nm.

The interactions between NPs and target cells depend greatly on the chemical and physical features of NPs, including their size, shape, and dispersion as well as their agglomeration form [59]. The shape, size, distribution, and morphology examinations of plant-mediated ultrasound-assisted synthesized CuO NPs were performed by SEM and TEM. The CuO NPs are embedded in the Mat/PEG matrix, with an average size of less than 100 nm and a homogenous distribution, as shown by the SEM image in Fig. 4. However, there is evidence of agglomeration. This agglomeration may have arisen due to the drying and vacuum steps during the preparation of the samples for SEM, as well as the layer-by-layer deposition of small particle sizes of CuO NPs with a hierarchical spherical structure. The TEM result (Fig. 5), reveals that the synthesized CuO NPs have a spherical form, with dimensions less than about 10 nm and a relatively homogeneous distribution. The image indicates that the NPs have a polydisperse distribution, comprising particles of different sizes, and that there is no aggregation. The Mat/PEG matrix provides adequate stabilization for CuO NPs. Previous studies on

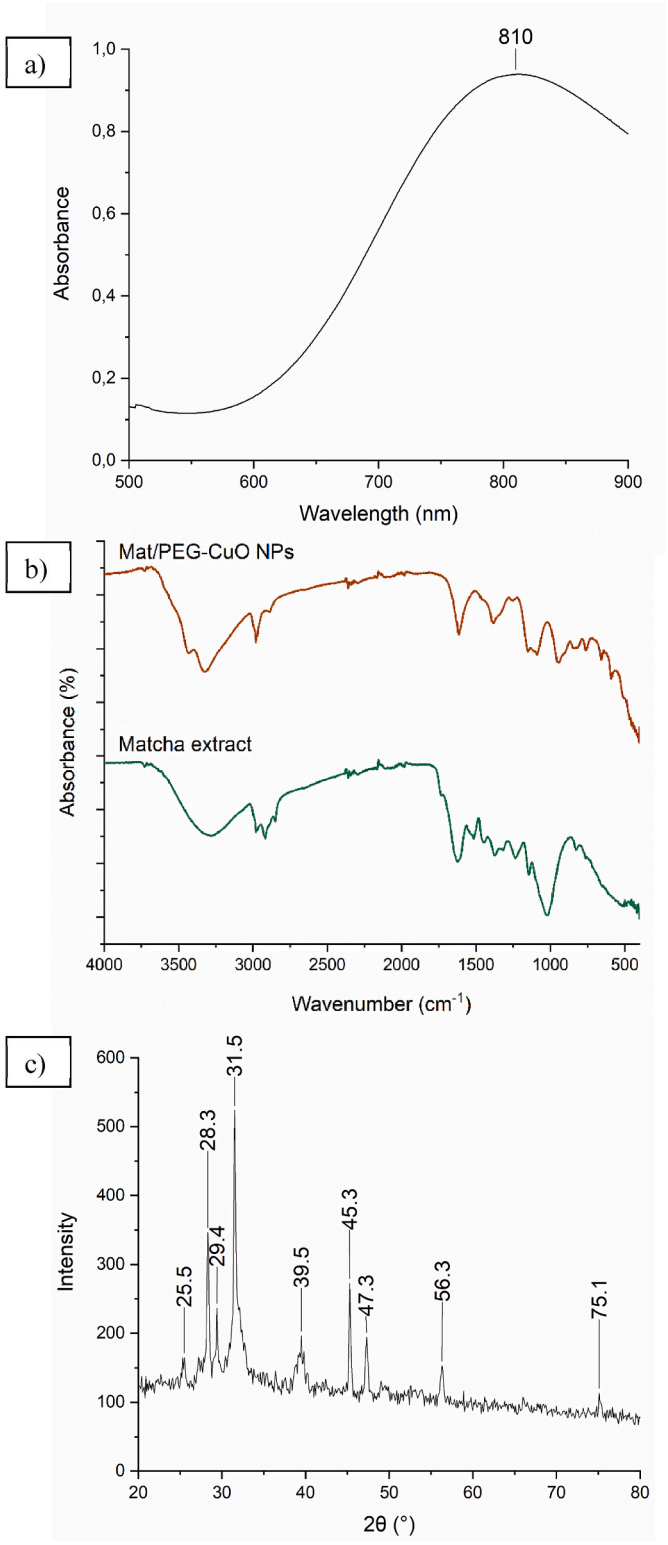


Fig. 3. a) UV–Vis, b) FTIR, and c) XRD spectrum of the phyto/sonosynthesized Mat/PEG-CuO NPs.

plant-mediated synthesized CuO NPs [17,60,61] reported similar findings.

3.2. Characterization results of Mat/PEG-CuO NPs coated SS316L

The surface of SS316L has been modified with plant-mediated ultrasound-assisted synthesized CuO NPs using a fast, inexpensive, and simple airbrush spray coating technique. Fig. 6 shows SEM results of the CuO NPs coated surface at various magnifications. As shown, the coating fully covers the surface of the SS316L while maintaining the particle structure of the CuO NPs. In addition, the CuO NPs on the surface have a spherical shape, have a size of about 50–70 nm, and show a homogeneous distribution. Looking at the image in the close-up (Fig. 6b), it has been noted that the CuO NPs are clustered in places. In the study by Tavakoli et al., it was stated that CuO NPs agglomerated locally on SS316L but offered multifunctional properties by roughening the surface [25]. In addition, the cutting lines created during the CNC cutting of the SS316L bar are clearly visible. As a result of the examination of the surface morphologies of Mat/PEG-CuO NPs coated SS316L at different magnifications, it is seen that the coating is mono-layered and rough, and no defects or cracks were observed on the surface.

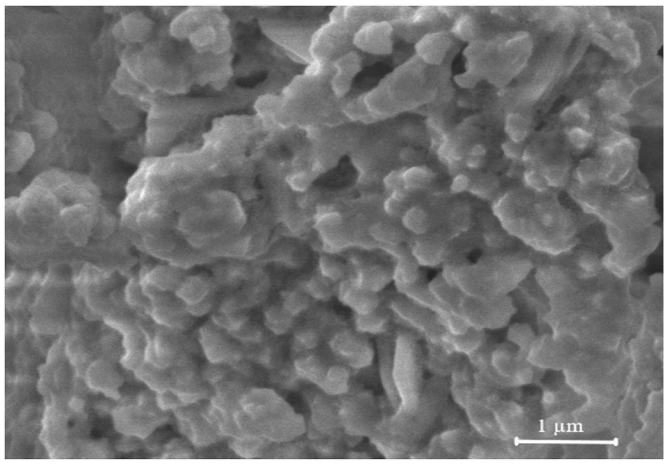


Fig. 4. SEM result of the phyto/sonosynthesized Mat/PEG-CuO NPs.

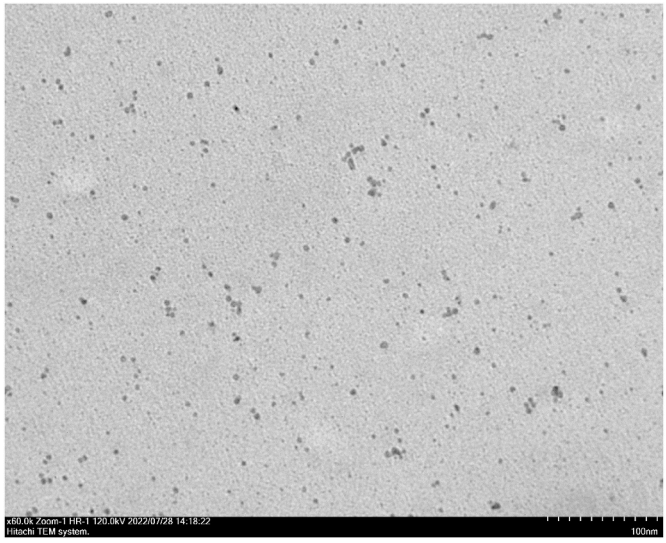


Fig. 5. TEM result of the phyto/sonosynthesized Mat/PEG-CuO NPs.

The cross-sectional view of the coating surface, the distribution of the CuO NPs coating on the SS316L surface, and whether it forms a metallurgical bond with the substrate material were examined by optical microscope. As seen in Fig. 7a, the surfaces coated using airbrush spray technique have no porosities and the coating was homogeneously distributed on the surface. The solution of CuO NPs completely covers the surface of the SS316L and there is no interaction with the substrate material. As a result of the optical microscopy examination, the mean thickness was found to be 8.773 µm.

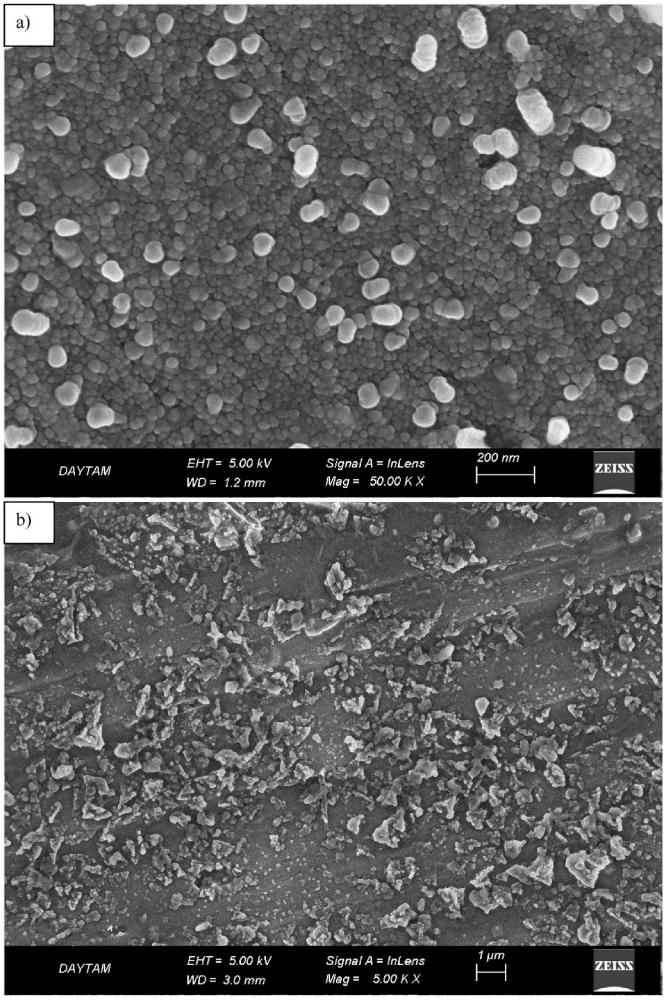


Fig. 6. SEM results of the Mat/PEG-CuO NPs coated SS316L with different magnifications: a) ×50.000 and b) x5.000.

To investigate the distribution of NPs on the coated surface in 3D and to measure the coating thickness accurately, 3D imaging was performed using a profilometer. In the 3D image in Fig. 7b, the black areas represent the deepest region on the coated surface, while the white areas represent the highest region. In the 3D profile, the cutting lines created during CNC cutting are clearly visible. The 3D profile is compatible with the SEM images. The coating thickness tests carried out with a profilometer show that the coating thickness is 5.31 µm.

The surface roughness of biometallic materials is important for cell adhesion, proliferation, and growth. The change in average surface roughness after coating was investigated and the results are shown in Table 2. In the literature, the surface roughness values of metallic materials to be used as biomaterials are classified as fine (0.5–1 µm) and medium (1–2 µm) [62]. While the value of the average surface roughness of the uncoated sample was 1.287 µm, the value of the coated surface decreased to 1.066 µm (approx. %12). The main cause for the decrease in the surface roughness value here is that the coating is carried out with NPs and the measurement is made on a microns scale. As can be seen in the SEM (Fig. 6b) and 3D profile (Fig. 7b) images, the micron-scaled cutting lines on the surface were filled with NPs, resulting in a decrease in surface roughness. After coating, the surface roughness value of 1.066 µm shows that it is suitable for biometallic materials with a fine surface roughness value.

3.2.1. Electrochemical corrosion test result

The investigation of antibacterial and anticorrosion properties and biocompatibility of NPs is very important in terms of application areas. However, only a few studies reported on the biocompatibility of the coating of CuO NPs on the metallic surface [25,63]. Future research is needed to provide a detailed and systematic overview of the effects of coating CuO NPs on biometallic surfaces on biological properties. SS316L has corrosion resistance on the steel surface, with the passive layer formed by the contained Cr. In addition, it has improved corrosion properties as it contains 17–19%wt. Ni and 2.25–3%wt. Mo. In addition, the low carbon content (less than 0.03%wt.), marked "L", reduces the probability of chromium carbide formation, which further improves corrosion properties [1,64,65]. However, if this layer is damaged, it is very prone to corrosion (pitting or crevice) [66]. Therefore, corrosion resistance can be improved by coating a more passive layer on the surface. In this study, the effect of synthesized CuO NPs by matcha tea extract on the corrosion resistance of SS316L was determined by electrochemical corrosion measurements in Ringer's solution. First, the OCP values of bare and CuO NPs coated SS316L were measured. These values provide information about the inert behavior of the samples in the current medium [67]. Fig. 8a shows the OCP curves of bare and CuO NPs coated SS316L in Ringer's solution. As can be seen in Fig. 8a, the sample coated with CuO NPs showed more inert behavior than the bare sample throughout the experiment. It was observed that the coated samples in Ringer's solution were more stable by showing a value of −0.48 V compared to the bare samples (−0.61 V). After the OCP measurements, the electrochemical corrosion behavior was investigated by applying a cyclic potential. Fig. 8b shows the Tafel curves obtained as a result of the electrochemical corrosion tests. The corrosion potential of the SS316L coated with CuO NPs (−0.41 V) was significantly different from the bare SS316L (−0.53 V) on the Tafel curves, showing a shift in the left direction. Also, the Tafel plot showed that the surface-modified SS316L had a significantly lower current density (2.3×10^{-7} A cm^{-2}) than the bare substrate (3.4×10^{-6} A cm^{-2}). As can be seen from the result, the CuO NPs coating significantly enhanced the corrosion resistance of the substrate material. It is found that coating with Mat/PEG-CuO NPs created a new protective film on the surface of SS316L. In the study by Tavakoli et al. [25] on the coating containing CuO NPs, it was stated that the presence of CuO NPs on the surface of SS316L increases corrosion resistance. However, the situation was found to vary at different rates of CuO NPs. The anti-corrosive coating with Mat/PEG-CuO NPs obtained in the present study is consistent with this study. In another study by Zhang et al. [13], it was stated that the coatings prepared by adding silver NPs (Ag NPs) to the polytetrafluoroethylene (PTFE) layer increased the corrosion resistance. After comparing the Tafel curves, it was found that the coating with Mat/PEG-CuO NPs increased the corrosion resistance of SS316L substrate more. The research on the corrosion resistance of various NPs coatings used on the SS316L surface is summarized in Table 3.

3.2.2. Antibacterial activity results

Post-implant reactions are typically brought on by the efficiency with which bacteria bind to the surface of metallic biomaterials, which results in the development of a biofilm, which provides a variety of difficulties for the host [69]. For this reason, the antibacterial properties of SS316L, which is often preferred as a metallic bioimplant material, need to be improved. In the literature, Ag NP-based coatings come to the fore as an antibacterial agent [42,47]. It is known that Cu-based nanostructures have antibacterial properties [49–51,70]. In this study, the antibacterial properties of plant-mediated ultrasound-assisted synthesized CuO NPs were investigated after coating on the SS316L surface by airbrush spraying technique for the first time. The agar well diffusion technique was used to evaluate the antibacterial behavior of the prepared coated surfaces against *E. coli* and *S. aureus* species. Fig. 9 shows the antibacterial behavior of the uncoated SS316L (Fig. 9a) and the SS316L coated with CuO NPs (Fig. 9b) is given with *E. coli* on the left and *S. aureus* on the right. Uncoated samples showed no antibacterial behavior with either bacterial species. As shown in Fig. 9b, the Mat/PEG-CuO NPs coating has an antibacterial activity for both species. It showed a ZOI of

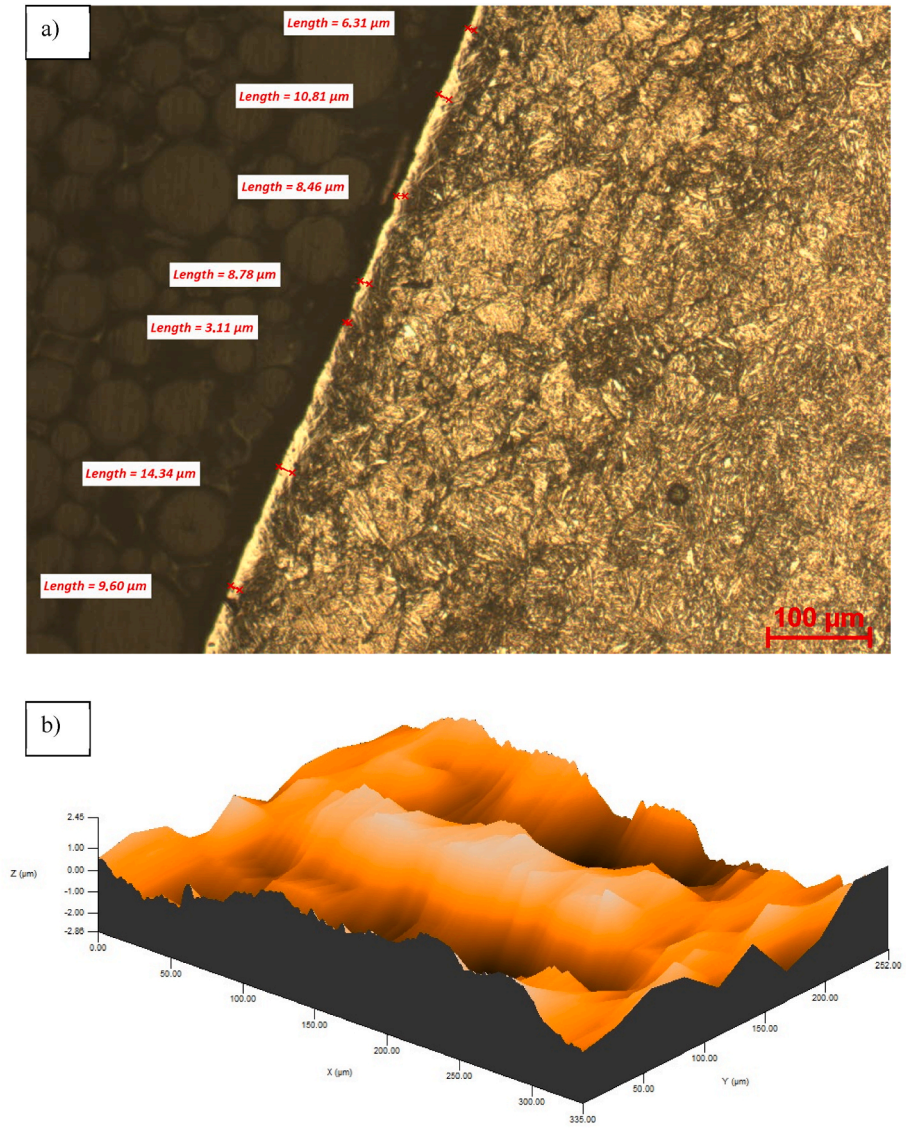


Fig. 7. a) Cross-sectional view and b) 3D surface profile of CuO NPs coated samples.

Table 2
Average surface roughness values of specimens.

Specimen	Average Surface Roughness (Ra, μm)
Uncoated	1.287
Mat/PEG-CuO NPs coated	1.066

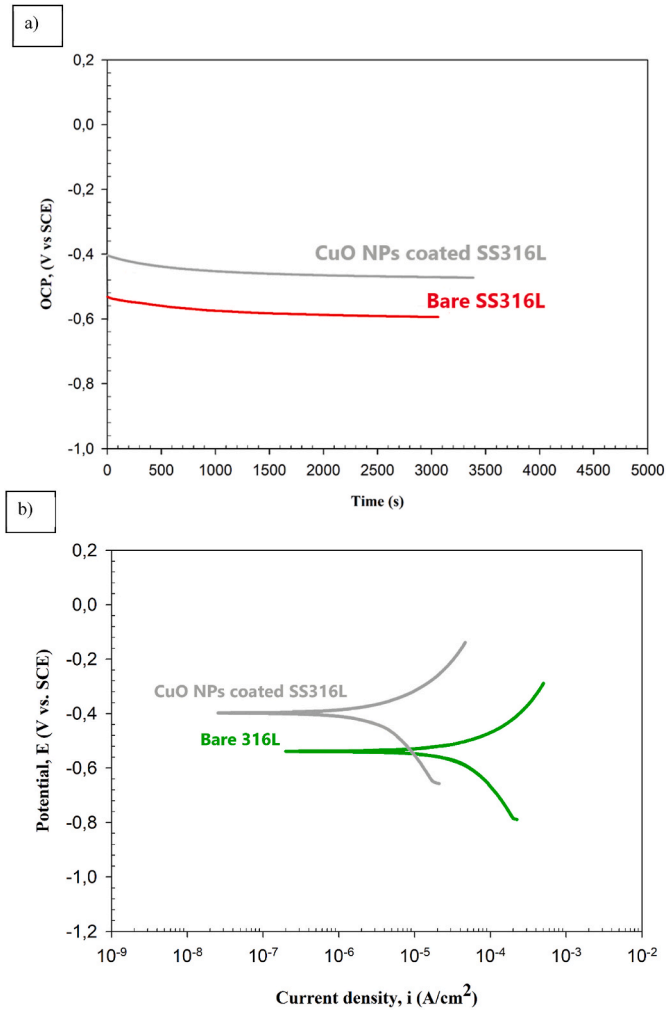


Fig. 8. Electrochemical corrosion test results a) OCP and b) Tafel curves.

29.5 mm against the gram-negative strain *E. coli* and 25.5 mm against the gram-positive strain *S. aureus*. A more active behavior was observed against the *E. coli* strain. Antibacterial metal-based NPs directly or indirectly cause the death of pathogens by destroying the cell wall and inhibiting RNA synthesis or DNA replication [51]. Previous investigations suggested that the generation of reactive oxygen species (ROS) and the release of metal ions may be the primary causes of CuO's antibacterial activity against both gram-negative and gram-positive species [71]. The ROS, which consist of the hydroxyl (-OH) and superoxide (O^{2-}) radicals generated by CuO, enter the microorganism and damage its DNA, proteins, lipids, and amino acids, as well as destroying its cells [72]. These ROS have the potential to damage phospholipid double bonds, increasing the fluidity of the membrane and making cells more vulnerable to osmosis. Iron-sulfur cluster that serve as cofactors for enzymes can also sustain damage from ROS. The antimicrobial properties of CuO may also be linked to the release of copper ions, which may form complexes with the bacteria's components and harm their proteins and cell walls [73]. Additionally, Cu ions have a relationship with DNA that predominantly inhibits bacterial proliferation. CuO exhibits a potent lethal agent against pathogenic microorganisms as a result of all these features. Compared to CuO NPs synthesized through plant-mediated methods in prior literature, the current study found a significantly higher ZOI value, indicating superior antibacterial properties. These enhancements in both antibacterial and anticorrosive properties highlight the suitability of the CuO NPs for a range of multifunctional environmental, energy and medical applications. Comprehensive studies are essential for the effective use of plant-mediated CuO NPs in many areas. The further objectives of this study will be to expand the scope of the study.

3.3. Contribution of this study to an eco-sustainable green approach

The aim of a sustainable and green approach is the design of chemical products that eliminate the use of substances that pose a danger to the environment and humans, within greater social expectations, and a sustainable global future of the world. Fig. 10 shows the principles of the eco-sustainable green approach. The green approach aims at processes for the production of products that are safe, energy-efficient and minimize greenhouse gas emissions. Sustainable and green approaches are about environmentally sustainable production processes. The conventional methods (physical and chemical approaches) for synthesizing NPs have significant disadvantages related to high cost (in terms of energy, resources, area, and time) and human-environmental toxicity. Therefore, there was a requirement to develop an alternative synthesis route with green synthesis methodology. In general, green synthesis involves using biological resources such as fungi, plants or bacteria to synthesize ecologically safe and biocompatible NPs. The biological methods generally involves facile scaling without high temperature, pressure, toxic chemicals and uses environment-friendly and cost-effective resources. Another advantage is that it can be easily produced without the use of harmful chemicals for large-scale production. With specific interactions between inorganic materials and biomolecules, these biological methods can easily result in NPs of controlled shape and size. It includes the green approach as bio reducers are used to seal and stabilize the agents without using plant extracts or renewable microorganisms, additional chemical reagents. The green synthesis of NPs aims to minimize the waste produced and implement sustainability [74,75]. Research investment and teamwork are needed to improve the sustainable and green approach in the synthesis and applications of NPs. Main aim of this study is to highlight the biological synthesis of metal-based NPs, thanks to their rapid production and eco-friendly synthesis convenience. Using biological sources, this study addressed an environmentally friendly way of producing metal-based NPs from the synthesis and characterization of plant-mediated NPs. All the processes in this study are environmentally

Table 3
The studies examining the corrosion behavior of SS316L surface coated with NPs.

Coating	Coating Technique	Test Medium	Result	References
PDMS/SiO_2/CuO NPs	Dip coating	Simulated body fluid (SBF)	Improvement in resistance	Tavakoli et al. [25]
Ag NPs/PTFE	Sol-gel dip coating	Phosphate-buffered saline (PBS)	Improvement in resistance	Zhang et al. [13]
Chitosan-Copper NPs	Electrophoretic deposition	Simulated body fluid (SBF)	Improvement in resistance	Tabesh et al. [63]
Polydopamine/Ag NPs	Dip coating	NaCl solution	Decrease in resistance	Qian et al. [68]
Locust/PEG-Ag NPs	Airbrush spray coating	Ringer solution	Improvement in resistance	Karabulut et al. [47]
Mat/PEG-CuO NPs	Airbrush spray coating	Ringer solution	Improvement in resistance	Present study

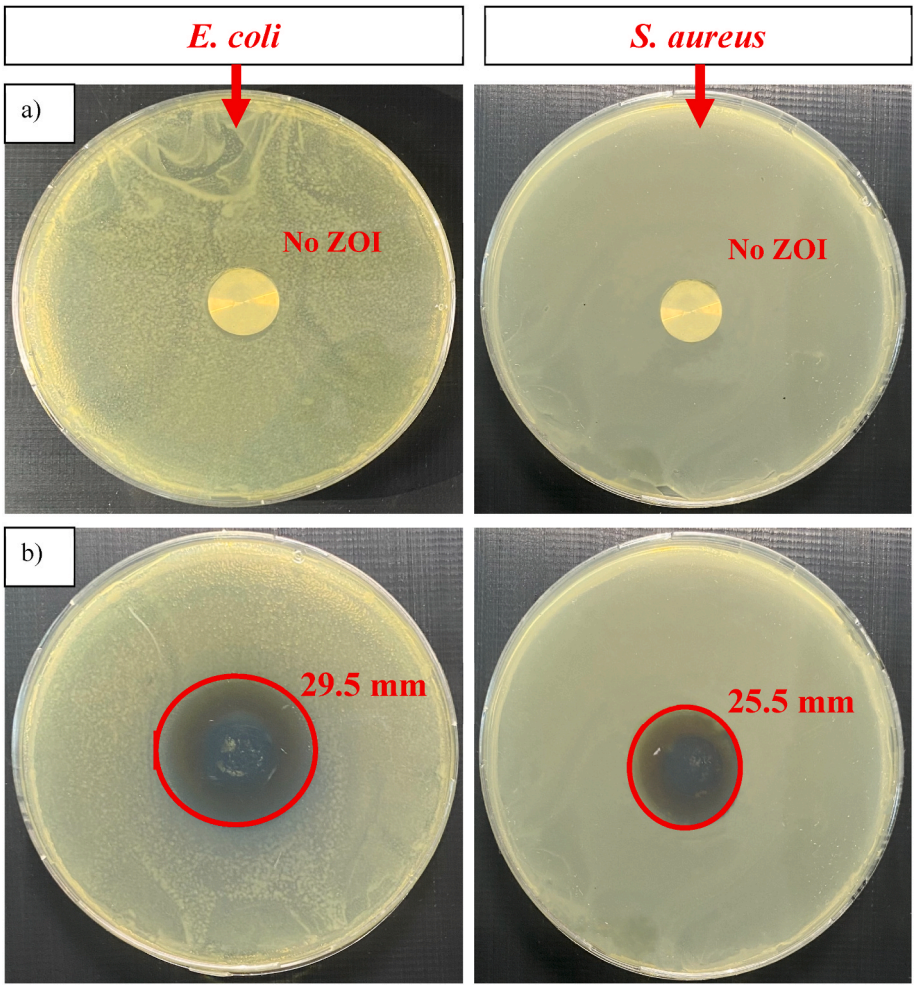


Fig. 9. Antibacterial activity test results a) uncoated b) Mat/PEG-CuO NPs coated samples.



Fig. 10. The principles of eco-sustainable green approach. (For interpretation of the references to colour in this figure legend, the reader is referred to the Web version of this article.)

friendly green techniques; the synthesis method of CuO NPs and coating technique used for substrates [47].

4. Conclusion

The main objective of this research was to prepare an antibacterial and anticorrosive coating on the surface of SS316L using extract-based synthesized Mat/PEG-CuO NPs. The synthesized CuO NPs and novel nanostructures coating on the surface of SS316L were characterized by multifaceted investigations. The results of the present study are as follows:

- The CuO NPs have a size of less than 10 nm and consist of polydisperse distribution with a regular morphology and spherical shape in the Mat/PEG matrix.
- Surface roughness values of superficially modified SS316L have slightly decreased. It has approached in classification from medium to fine and is more suitable for use in metallic biomaterials.
- A uniform transition interface without crack or delamination was formed between the surface of SS316L and CuO NPs coating. The coating thickness is very close, and all the coating is in a single-layer.
- The corrosion resistance of CuO NPs coated on SS316L is significantly higher than uncoated SS316L.
- The antibacterial activity of CuO NPs coated on SS316L was expressed as the diameter of the zone of inhibition. The surface modified SS316L exhibited significant inhibitory zones of 29.5 for *E. coli* and 25.5 mm for *S. aureus* test organisms compared with uncoated ones.

- The results demonstrated that the antibacterial and anticorrosive properties of the surface modified SS316L were better compared to the bare substrate. These results are promising for use in the medical field.
- It has significant potential to be a promising nanocoating of the SS316L applicability in the biomedical field due to the inexpensive, simple, fast, and eco-friendly of all production stages.
- Biocompatibility is a crucial design criterion for CuO NPs use in human life. Improved biocompatibility by changing the surface properties of metallic biomaterials may provide promising information for multifunctional applications of metallic nanomaterials.
- This study demonstrates that the green synthesis of plant-based synthesis of CuO NPs is an advantageous alternative to chemical and physical approaches.

Funding

This study was funded by Scientific Research Projects Coordination Unit of Istanbul University-Cerrahpaşa. Project number: FYL-2021-36085.

CRediT authorship contribution statement

Gizem Karabulut: Writing – review & editing, Methodology, Visualization. **Nuray Beköz Üllen:** Writing – review & editing, Supervision, Project administration. **Selcan Karakuş:** Writing – review & editing, Visualization, Methodology, Resources. **Ceyhun Toruntay:** Methodology, Writing.

Declaration of competing interest

The authors declare that they have no known competing financial interests or personal relationships that could have appeared to influence the work reported in this paper.

Data availability

Data will be made available on request.

References

[1] T. Hanawa, Overview of metals and applications, Met. Biomed. Devices (2019) 3–29, https://doi.org/10.1016/B978-0-08-102666-3.00001-8.
[2] J. Wilson, Metallic biomaterials, Fundam. Biomater. Met (2018) 1–33, https://doi.org/10.1016/B978-0-08-102205-4.00001-5.
[3] E.P. Ivanova, K. Bazaka, R.J. Crawford, New functional biomaterials for medicine and healthcare, New Funct. Biomater. Med. Healthc. (2014) 1–226, https://doi.org/10.1533/9781782422662.
[4] P. Kumar, N. Duraipandy, K. Manikantan Syamala, N. Rajendran, Antibacterial effects, biocompatibility and electrochemical behavior of zinc incorporated niobium oxide coating on 316L SS for biomedical applications, Appl. Surf. Sci. 427 (2018) 1166–1181, https://doi.org/10.1016/J.APSUSC.2017.08.221.
[5] M. Kumar, R. Kumar, S. Kumar, Coatings on orthopedic implants to overcome present problems and challenges: a focused review, Mater. Today Proc. 45 (2021) 5269–5276, https://doi.org/10.1016/J.MATPR.2021.01.831.
[6] M.A. Garcia-Lobato, A.I. Mtz-Enriquez, C.R. Garcia, M. Velazquez-Manzanares, F. Avalos-Belmontes, R. Ramos-Gonzalez, L.A. Garcia-Cerda, Corrosion resistance and in vitro bioactivity of dense and porous titania coatings deposited on 316L SS by spraying method, Appl. Surf. Sci. 484 (2019) 975–980, https://doi.org/10.1016/J.APSUSC.2019.04.108.
[7] M. Mathina, E. Shinyjoy, S. Ramya, L. Kavitha, D. Gopi, Multifunctional crab shell derived hydroxyapatite/metal oxide/polyhydroxybutyrate composite coating on 316L SS for biomedical applications, Mater. Lett. 313 (2022), 131701, https://doi.org/10.1016/J.MATLET.2022.131701.
[8] K. Xue, L.X. Liang, S.C. Cheng, H.P. Liu, L.Y. Cui, R.C. Zeng, S.Q. Li, Z.L. Wang, Corrosion resistance, antibacterial activity and drug release of ciprofloxacin-loaded micro-arc oxidation/silane coating on magnesium alloy AZ31, Prog. Org. Coating 158 (2021), 106357, https://doi.org/10.1016/J.PORGCOAT.2021.106357.
[9] R. Ahmadi, N. Asadpourchallou, B.K. Kaleji, In vitro study: evaluation of mechanical behavior, corrosion resistance, antibacterial properties and biocompatibility of HAp/TiO2/Ag coating on Ti6Al4V/TiO2 substrate, Surface. Interfac. 24 (2021), 101072, https://doi.org/10.1016/J.SURFIN.2021.101072.
[10] S.T. Chen, H.W. Chien, C.Y. Cheng, H.M. Huang, T.Y. Song, Y.C. Chen, C.H. Wu, Y. H. Hsueh, Y.H. Wang, S.F. Ou, Drug-release dynamics and antibacterial activities of chitosan/cefazolin coatings on Ti implants, Prog. Org. Coating 159 (2021), 106385, https://doi.org/10.1016/J.PORGCOAT.2021.106385.
[11] L. Li, Y. Wang, K. Liu, L. Yang, B. Zhang, Q. Luo, R. Luo, Y. Wang, Nanoparticles-stacked superhydrophilic coating supported synergistic antimicrobial ability for enhanced wound healing, Mater. Sci. Eng., C 132 (2022), 112535, https://doi.org/10.1016/J.MSEC.2021.112535.
[12] A. Santos-Coquillat, E. Martínez-Campos, H. Mora Sánchez, L. Moreno, R. Arrabal, M. Mohedano, A. Gallardo, J. Rodríguez-Hernández, E. Matykina, Hybrid functionalized coatings on metallic biomaterials for tissue engineering, Surf. Coating. Technol. 422 (2021), 127508, https://doi.org/10.1016/J.SURFCOAT.2021.127508.
[13] S. Zhang, X. Liang, G.M. Gadd, Q. Zhao, A sol–gel based silver nanoparticle/polytetrafluorethylene (AgNP/PTFE) coating with enhanced antibacterial and anti-corrosive properties, Appl. Surf. Sci. 535 (2021), 147675, https://doi.org/10.1016/J.APSUSC.2020.147675.
[14] S. Velumani, G. Regmi, M. Lee, H. Castaneda, M. Kuttolamadom, X. Qian, A. Kassiba, Engineered Zr/Zn/Ti oxide nanocomposite coatings for multifunctionality, Appl. Surf. Sci. 563 (2021), 150353, https://doi.org/10.1016/J.APSUSC.2021.150353.
[15] A. Waris, M. Din, A. Ali, M. Ali, S. Afridi, A. Baset, A. Ullah Khan, A comprehensive review of green synthesis of copper oxide nanoparticles and their diverse biomedical applications, Inorg. Chem. Commun. 123 (2021), 108369, https://doi.org/10.1016/J.INOCHE.2020.108369.
[16] R.R. Pillai, P.B. Sreelekshmi, A.P. Meera, Enhanced biological performance of green sythesized copper oxide nanoparticles using Pimenta dioica leaf extract, Mater. Today Proc. 50 (2022) 163–172, https://doi.org/10.1016/J.MATPR.2021.11.547.
[17] A. Badri, S. Slimi, M. Guergueb, H. Kahri, X. Mateos, Green synthesis of copper oxide nanoparticles using Prickly Pear peel fruit extract: characterization and catalytic activity, Inorg. Chem. Commun. 134 (2021), 109027, https://doi.org/10.1016/J.INOCHE.2021.109027.
[18] Y. Lv, J. Liu, Z. Zhang, W. Zhang, A. Wang, F. Tian, W. Zhao, J. Yan, Green synthesis of CuO nanoparticles-loaded ZnO nanowires arrays with enhanced photocatalytic activity, Mater. Chem. Phys. 267 (2021), 124703, https://doi.org/10.1016/J.MATCHEMPHYS.2021.124703.
[19] L. Volfová, S. Andrei Irimiciuc, S. Chertopalov, P. Hruška, J. Čížek, M. Vondráček, M. Novotný, M. Butterling, M.O. Liedke, A. Wagner, J. Lancok, Tailoring pulsed laser deposition fabricated copper oxide film by controlling plasma parameters, Appl. Surf. Sci. 608 (2023), 155128, https://doi.org/10.1016/J.APSUSC.2022.155128.
[20] S. Lin, A.A. Taylor, Z. Ji, C.H. Chang, N.M. Kinsinger, W. Ueng, S.L. Walker, A. E. Nel, Understanding the transformation, speciation, and hazard potential of copper particles in a model septic tank system using zebrafish to monitor the effluent, ACS Nano 9 (2015) 2038–2048, https://doi.org/10.1021/NN507216F/SUPPL_FILE/NN507216F_SI_001.PDF.
[21] S. Lin, Y. Zhao, T. Xia, H. Meng, Z. Ji, R. Liu, S. George, S. Xiong, X. Wang, H. Zhang, S. Pokhrel, L. Mädler, R. Damoiseaux, S. Lin, A.E. Nel, High content screening in zebrafish speeds up hazard ranking of transition metal oxide nanoparticles, ACS Nano 5 (2011) 7284–7295, https://doi.org/10.1021/NN202116P/SUPPL_FILE/NN202116P_SI_001.PDF.
[22] H. Zhang, Z. Ji, T. Xia, H. Meng, C. Low-Kam, R. Liu, S. Pokhrel, S. Lin, X. Wang, Y. P. Liao, M. Wang, L. Li, R. Rallo, R. Damoiseaux, D. Telesca, L. Mädler, Y. Cohen, J. I. Zink, A.E. Nel, Use of metal oxide nanoparticle band gap to develop a predictive paradigm for oxidative stress and acute pulmonary inflammation, ACS Nano 6 (2012) 4349–4368, https://doi.org/10.1021/NN3010087/SUPPL_FILE/NN3010087_SI_001.PDF.
[23] A.S. Adeleye, S. Pokhrel, L. Mädler, A.A. Keller, Influence of nanoparticle doping on the colloidal stability and toxicity of copper oxide nanoparticles in synthetic and natural waters, Water Res. 132 (2018) 12–22, https://doi.org/10.1016/J.WATRES.2017.12.069.
[24] H. Naatz, B.B. Manshian, C.R. Luci, V. Tsikourkitoudi, Y. Deligiannakis, J. Birkenstock, S. Pokhrel, L. Mädler, S.J. Soenen, Model-based nanoengineered pharmacokinetics of iron-doped copper oxide for nanomedical applications, Angew. Chem. 132 (2020) 1844–1852, https://doi.org/10.1002/ANGE.201912312.
[25] S. Tavakoli, S. Nemati, M. Kharaziha, S. Akbari-Alavijeh, Embedding CuO nanoparticles in PDMS-SiO2 coating to improve antibacterial characteristic and corrosion resistance, Colloid Interface Sci. Commun. 28 (2019) 20–28, https://doi.org/10.1016/J.COLCOM.2018.11.002.
[26] M. Ghashghaee, M. Fallah, A. Rabiee, Superhydrophobic nanocomposite coatings of poly(methyl methacrylate) and stearic acid grafted CuO nanoparticles with photocatalytic activity, Prog. Org. Coating 136 (2019), 105270, https://doi.org/10.1016/J.PORGCOAT.2019.105270.
[27] T. Abiraman, E. Ramanathan, G. Kavitha, R. Rengasamy, S. Balasubramanian, Synthesis of chitosan capped copper oxide nanoleaves using high intensity (30 kHz) ultrasound sonication and their application in antifouling coatings, Ultrason. Sonochem. 34 (2017) 781–791, https://doi.org/10.1016/J.ULTSONCH.2016.07.013.
[28] K. Velsankar, S. Suganya, P. Muthumari, S. Mohandoss, S. Sudhahar, Ecofriendly green synthesis, characterization and biomedical applications of CuO nanoparticles synthesized using leaf extract of Capsicum frutescens, J. Environ. Chem. Eng. 9 (2021), https://doi.org/10.1016/J.JECE.2021.106299.
[29] B. Bai, S. Saranya, V. Dheepaasri, S. Muniasamy, N.S. Alharbi, B. Selvaraj, V. S. Undal, B.M. Gnanamangai, Biosynthesized copper oxide nanoparticles (CuO

NPs) enhances the anti-biofilm efficacy against K. pneumoniae and S. aureus, J. King Saud Univ. Sci. 34 (2022), 102120, https://doi.org/10.1016/J.JKSUS.2022.102120.
[30] L.A. Kolahalam, K.R.S. Prasad, P.M. Krishna, N. Supraja, S. Shanmugan, The exploration of bio-inspired copper oxide nanoparticles: synthesis, characterization and in-vitro biological investigations, Heliyon 8 (2022), e09726, https://doi.org/10.1016/J.HELIYON.2022.E09726.
[31] K.R. Shubhashree, R. Reddy, A.K. Gangula, G.S. Nagananda, P.K. Badiya, S. S. Ramamurthy, P. Aramwit, N. Reddy, Green synthesis of copper nanoparticles using aqueous extracts from Hyptis suaveolens (L.), Mater. Chem. Phys. 280 (2022), 125795, https://doi.org/10.1016/j.matchemphys.2022.125795.
[32] S.V. Chakka, N. Thanjavur, S. Lee, S. Kim, Synthesis and characterization of lanthanum-doped curcumin-functionalized antimicrobial copper oxide nanoparticles, J. Rare Earths (2022), https://doi.org/10.1016/J.JRE.2022.08.020.
[33] S. Janaki, K. Punithamurthy, The influence of graphene oxide on structural, optical, and catalytic properties of LaFeO3 nanoparticles synthesized by hydrothermal method, Chem. Data Collect. 42 (2022), 100968, https://doi.org/10.1016/J.CDC.2022.100968.
[34] D. Rana, B.M. Mandal, S.N. Bhattacharyya, Analogue calorimetric studies of blends of poly(vinyl ester)s and polyacrylates, Macromolecules 29 (1996) 1579–1583, https://doi.org/10.1021/MA950954N/ASSET/IMAGES/MEDIUM/MA950954NE00004.GIF.
[35] D. Rana, B.M. Mandal, S.N. Bhattacharyya, Miscibility and phase diagrams of poly (phenyl acrylate) and poly(styrene-co-acrylonitrile) blends, Polymer 34 (1993) 1454–1459, https://doi.org/10.1016/0032-3861(93)90861-4.
[36] D. Rana, B.M. Mandal, S.N. Bhattacharyya, Analogue calorimetry of polymer blends: poly(styrene-co-acrylonitrile) and poly(phenyl acrylate) or poly(vinyl benzoate), Polymer 37 (1996) 2439–2443, https://doi.org/10.1016/0032-3861(96)85356-0.
[37] D. Rana, K. Bag, S.N. Bhattacharyya, B.M. Mandal, Miscibility of poly(styrene-co-butyl acrylate) with poly(ethyl methacrylate): existence of both UCST and LCST, J. Polym. Sci. B Polym. Phys. 38 (2000) 369–375, https://doi.org/10.1002/(SICI)1099-0488(20000201)38:3.
[38] Y. Cai, X. Luo, M. Maclean, Y. Qin, M. Duxbury, F. Ding, A single-step fabrication approach for development of antimicrobial surfaces, J. Mater. Process. Technol. 271 (2019) 249–260, https://doi.org/10.1016/J.JMATPROTEC.2019.04.012.
[39] E. De Giglio, D. Cafagna, S. Cometa, A. Allegretta, A. Pedico, L.C. Giannossa, L. Sabbatini, M. Mattioli-Belmonte, R. Iatta, An innovative, easily fabricated, silver nanoparticle-based titanium implant coating: development and analytical characterization, Anal. Bioanal. Chem. 405 (2013) 805–816, https://doi.org/10.1007/s00216-012-6293-z.
[40] D.A. Robinson, R.W. Griffith, D. Shechtman, R.B. Evans, M.G. Conzemius, In vitro antibacterial properties of magnesium metal against Escherichia coli, Pseudomonas aeruginosa and Staphylococcus aureus, Acta Biomater. 6 (2010) 1869–1877, https://doi.org/10.1016/J.ACTBIO.2009.10.007.
[41] A. Sharifnabi, M.H. Fathi, B. Eftekhari Yekta, M. Hossainalipour, The structural and bio-corrosion barrier performance of Mg-substituted fluorapatite coating on 316L stainless steel human body implant, Appl. Surf. Sci. 288 (2014) 331–340, https://doi.org/10.1016/J.APSUSC.2013.10.029.
[42] K. Jeeva Jothi, S. Balachandran, K. Palanivelu, Synergistic combination of Phyllanthus niruri/silver nanoparticles for anticorrosive application, Mater. Chem. Phys. 279 (2022), 125794, https://doi.org/10.1016/J.MATCHEMPHYS.2022.125794.
[43] A. Allion-Maurer, C. Saulou-Bérion, R. Briandet, S. Zanna, N. Lebleu, P. Marcus, P. Raynaud, B. Despax, M. Mercier-Bonin, Plasma-deposited nanocomposite polymer-silver coating against Escherichia coli and Staphylococcus aureus: antibacterial properties and ageing, Surf. Coating. Technol. 281 (2015) 1–10, https://doi.org/10.1016/J.SURFCOAT.2015.09.025.
[44] F.W. Abdulsada, A.S. Hammood, Characterization of corrosion and antibacterial resistance of hydroxyapatite/silver nano particles powder on 2507 duplex stainless steel, Mater. Today Proc. 42 (2021) 2301–2307, https://doi.org/10.1016/J.MATPR.2020.12.319.
[45] S.A. Gawad, A. Nasr, A.M. Fekry, L.O. Filippov, Electrochemical and hydrogen evolution behaviour of a novel nano-cobalt/nano-chitosan composite coating on a surgical 316L stainless steel alloy as an implant, Int. J. Hydrogen Energy 46 (2021) 18233–18241, https://doi.org/10.1016/J.IJHYDENE.2021.03.018.
[46] A.P.R. Alves Claro, R.T. Konatu, A.L. do A. Escada, M.C. de Souza Nunes, C. V. Maurer-Morelli, M.F. Dias-Netipanyj, K.C. Popat, D. Mantovani, Incorporation of silver nanoparticles on Ti7.5Mo alloy surface containing TiO2 nanotubes arrays for promoting antibacterial coating – in vitro and in vivo study, Appl. Surf. Sci. 455 (2018) 780–788, https://doi.org/10.1016/J.APSUSC.2018.05.189.
[47] G. Karabulut, N. Beköz Üllen, E. Akyüz, S. Karakuş, Surface modification of 316L stainless steel with multifunctional locust gum/polyethylene glycol-silver nanoparticles using different coating methods, Prog. Org. Coating 174 (2023), 107291, https://doi.org/10.1016/J.PORGCOAT.2022.107291.
[48] V.U. Siddiqui, A. Ansari, R. Chauhan, W.A. Siddiqi, Green synthesis of copper oxide (CuO) nanoparticles by Punica granatum peel extract, Mater. Today Proc. 36 (2021) 751–755, https://doi.org/10.1016/J.MATPR.2020.05.504.
[49] N. Anitha, N. Jayarambabu, A. Akshaykranth, T. Venkatappa Rao, Tinospora cordifoliaapproached copper oxide nanoparticles using different concentrations for optical and antibacterial applications, Inorg. Chem. Commun. 143 (2022), 109786, https://doi.org/10.1016/J.INOCHE.2022.109786.
[50] G. Sharmila, M. Thirumarimurugan, V.M. Sivakumar, Optical, catalytic and antibacterial properties of phytofabricated CuO nanoparticles using Tecoma castanifolia leaf extract, Optik 127 (2016) 7822–7828, https://doi.org/10.1016/J.IJLEO.2016.05.142.
[51] H.C.A. Murthy, T. Desalegn, M. Kassa, B. Abebe, T. Assefa, Synthesis of green copper nanoparticles using medicinal plant hagenia abyssinica (brace) JF. Gmel. Leaf extract: antimicrobial properties, J. Nanomater. 2020 (2020), https://doi.org/10.1155/2020/3924081.
[52] S. Basavaraja, S.D. Balaji, A. Lagashetty, A.H. Rajasab, A. Venkataraman, Extracellular biosynthesis of silver nanoparticles using the fungus Fusarium semitectum, Mater. Res. Bull. 43 (2008) 1164–1170, https://doi.org/10.1016/J.MATERRESBULL.2007.06.020.
[53] H. Joy Prabu, R. Varghese, I. Johnson, S. John Sundaram, A. Dhayal Raj, R. Rajagopal, P. Kuppusamy, R. Sathya, K. Kaviyarasu, Laser induced plant leaf extract mediated synthesis of CuO nanoparticles and its photocatalytic activity, Environ. Res. 212 (2022), https://doi.org/10.1016/J.ENVRES.2022.113295.
[54] E. Tan, İ.M. Kahyaoğlu, S. Karakuş, A sensitive and smartphone colorimetric assay for the detection of hydrogen peroxide based on antibacterial and antifungal matcha extract silver nanoparticles enriched with polyphenol, Polym. Bull. (2021) 1–27, https://doi.org/10.1007/S00289-021-03857-W/TABLES/5.
[55] S. Karakuş, G. Baytemir, C. Özeroğlu, N. Taşaltın, An ultra-sensitive smartphone-integrated digital colorimetric and electrochemical Camellia sinensis polyphenols encapsulated CuO nanoparticles-based ammonia biosensor, Inorg. Chem. Commun. 143 (2022), 109733, https://doi.org/10.1016/J.INOCHE.2022.109733.
[56] J.V.C. do Carmo, R. de C.F. Bezerra, S. Tehuacanero-Cuapa, E. Rodríguez-Aguado, R. Lang, A.F. Campos, G. Duarte, G.D. Saraiva, L. Otubo, A.C. Oliveira, E. Rodríguez-Castellón, Synthesis of tailored alumina supported Cu-based solids obtained from nanocomposites: catalytic application for valuable aldehyde and ketones production, Mater. Chem. Phys. 292 (2022), 126800, https://doi.org/10.1016/J.MATCHEMPHYS.2022.126800.
[57] A. Ahmad, M. Khan, S. Khan, R. Luque, K.M. Abualnaja, O.K. Alduaij, T.A. Yousef, Bio-construction of CuO nanoparticles using Texas sage plant extract for catalytical degradation of methylene blue via photocatalysis, J. Mol. Struct. 1256 (2022), 132522, https://doi.org/10.1016/J.MOLSTRUC.2022.132522.
[58] S. Rehman, A. Mumtaz, S.K. Hasanain, Size effects on the magnetic and optical properties of CuO nanoparticles, J. Nanoparticle Res. 13 (2011) 2497–2507, https://doi.org/10.1007/S11051-010-0143-8/FIGURES/12.
[59] T.A. Saleh, Nanomaterials: classification, properties, and environmental toxicities, Environ. Technol. Innov. 20 (2020), 101067, https://doi.org/10.1016/J.ETI.2020.101067.
[60] A. Karabatak, F. Danışman-Kalındemirtaş, E. Tan, S. Erdem-Kuruca, S. Karakuş, Kappa carrageenan/PEG-CuO nanoparticles as a multifunctional nanoplatform: digital colorimetric biosensor and anticancer drug nanocarrier, Appl. Phys. Mater. Sci. Process 128 (2022) 1–12, https://doi.org/10.1007/S00339-022-05802-8/FIGURES/7.
[61] M. Ilgar, G. Baytemir, N. Taşaltın, S. Güllülü, İ.S. Yeşilyurt, S. Karakuş, Multifunctional maca extract coated CuO nanoparticles with antimicrobial and dopamine sensing activities: a dual electrochemical – smartphone colorimetric detection system, J. Photochem. Photobiol. Chem. 431 (2022), 114075, https://doi.org/10.1016/J.JPHOTOCHEM.2022.114075.
[62] T. Albrektsson, A. Wennerberg, Oral implant surfaces: Part 1–review focusing on topographic and chemical properties of different surfaces and in vivo responses to them, Int. J. Prosthodont. (IJP) 17 (2004) 536–543.
[63] E. Tabesh, H.R. Salimijazi, M. Kharaziha, M. Mahmoudi, M. Hejazi, Development of an in-situ chitosan-copper nanoparticle coating by electrophoretic deposition, Surf. Coating. Technol. 364 (2019) 239–247, https://doi.org/10.1016/J.SURFCOAT.2019.02.040.
[64] E.P. Ivanova, K. Bazaka, R.J. Crawford, Metallic biomaterials: types and advanced applications, New Funct, Biomater. Med. Healthc (2014) 121–147, https://doi.org/10.1533/9781782422662.121.
[65] D. Zindani, K. Kumar, J. Paulo Davim, Metallic biomaterials-A review, Mech. Behav. Biomater (2019) 83–99, https://doi.org/10.1016/B978-0-08-102174-3.00004-8.
[66] V. Azar, B. Hashemi, M. Rezaee Yazdi, The effect of shot peening on fatigue and corrosion behavior of 316L stainless steel in Ringer's solution, Surf. Coating. Technol. 204 (2010) 3546–3551, https://doi.org/10.1016/J.SURFCOAT.2010.04.015.
[67] I. Mutlu, Characterisation of localised corrosion behaviour of Ti-Ta-Mo alloy for the nuclear industry, Corrosion Rev. 35 (2017) 13–21, https://doi.org/10.1515/CORRREV-2016-0051/MACHINEREADABLECITATION/RIS.
[68] H. Qian, M. Li, Z. Li, Y. Lou, L. Huang, D. Zhang, D. Xu, C. Du, L. Lu, J. Gao, Mussel-inspired superhydrophobic surfaces with enhanced corrosion resistance and dual-action antibacterial properties, Mater. Sci. Eng., C 80 (2017) 566–577, https://doi.org/10.1016/J.MSEC.2017.07.002.
[69] S.M. Emarati, M. Mozammel, Efficient one-step fabrication of superhydrophobic nano-TiO2/TMPSi ceramic composite coating with enhanced corrosion resistance on 316L, Ceram. Int. 46 (2020) 1652–1661, https://doi.org/10.1016/J.CERAMINT.2019.09.137.
[70] S. Logambal, C. Maheswari, S. Chandrasekar, T. Thilagavathi, C. Inmozhi, S. Panimalar, F.A. Bassyouni, R. Uthrakumar, M.R.A. Gawwad, R.M. Aljowaie, D. A. Al Farraj, K. Kanimozhi, Synthesis and characterizations of CuO nanoparticles using Couroupita guianensis extract for and antimicrobial applications, J. King Saud Univ. Sci. 34 (2022), 101910, https://doi.org/10.1016/J.JKSUS.2022.101910.
[71] A.A. Keller, A.S. Adeleye, J.R. Conway, K.L. Garner, L. Zhao, G.N. Cherr, J. Hong, J. L. Gardea-Torresdey, H.A. Godwin, S. Hanna, Z. Ji, C. Kaweeteerawat, S. Lin, H. S. Lenihan, R.J. Miller, A.E. Nel, J.R. Peralta-Videa, S.L. Walker, A.A. Taylor, C. Torres-Duarte, J.I. Zink, N. Zuverza-Mena, Comparative environmental fate and toxicity of copper nanomaterials, NanoImpact 7 (2017) 28–40, https://doi.org/10.1016/J.IMPACT.2017.05.003.

[72] M. Alavi, R.S. Varma, Phytosynthesis and modification of metal and metal oxide nanoparticles/nanocomposites for antibacterial and anticancer activities: recent advances, Sustain. Chem. Pharm. 21 (2021), 100412, https://doi.org/10.1016/J.SCP.2021.100412.

[73] G.M. Raghavendra, J. Jung, D. Kim, J. Seo, Chitosan-mediated synthesis of flowery-CuO, and its antibacterial and catalytic properties, Carbohydr. Polym. 172 (2017) 78–84, https://doi.org/10.1016/J.CARBPOL.2017.04.070.

[74] V. Soni, P. Raizada, P. Singh, H.N. Cuong, R. S, A. Saini, R.V. Saini, Q. Van Le, A. K. Nadda, T.T. Le, V.H. Nguyen, Sustainable and green trends in using plant extracts for the synthesis of biogenic metal nanoparticles toward environmental and pharmaceutical advances: a review, Environ. Res. 202 (2021), 111622, https://doi.org/10.1016/j.envres.2021.111622.

[75] S. AlNadhari, N.M. Al-Enazi, F. Alshehrei, F. Ameen, A review on biogenic synthesis of metal nanoparticles using marine algae and its applications, Environ. Res. 194 (2021), 110672, https://doi.org/10.1016/j.envres.2020.110672.